THE JOURNAL OF BIOLOGICAL CHEMISTRY
Vol. 276, No. 45, Issue of November 9, pp. 42293–42301, 2001
Printed in U.S.A.

Androgen-induced NH_2- and COOH-terminal Interaction Inhibits p160 Coactivator Recruitment by Activation Function 2*

Received for publication, August 6, 2001, and in revised form, September 6, 2001
Published, JBC Papers in Press, September 10, 2001, DOI 10.1074/jbc.M107492200

Bin He, Natalie T. Bowen, John T. Minges, and Elizabeth M. Wilson‡

From the Laboratories for Reproductive Biology, the Departments of Biochemistry and Biophysics, and the Department of Pediatrics, University of North Carolina, Chapel Hill, North Carolina 27599

The androgen receptor undergoes an androgen-specific NH_2- and COOH-terminal interaction between NH_2-terminal motif F*XX*LF and activation function 2 in the ligand binding domain. We demonstrated previously that activation function 2 forms overlapping binding sites for the androgen receptor F*XX*LF motif and the L*XX*LL motifs of p160 coactivators. Here we investigate the influence of the NH_2- and COOH-terminal interaction on androgen receptor function. Specificity and relative potency of the motif interactions were evaluated by ligand dissociation rate and the stability of chimeras of transcriptional intermediary factor 2 with full-length and truncated androgen or glucocorticoid receptor. The results indicate that the androgen receptor activation function 2 interacts specifically and with greater avidity with the single F*XX*LF motif than with the L*XX*LL motif region of p160 coactivators, whereas this region of the glucocorticoid receptor interacts preferentially with the L*XX*LL motifs. Expression of the L*XX*LL motifs as a fusion protein with the glucocorticoid receptor resulted in loss of agonist-induced receptor destabilization and increased half-time of ligand dissociation. The NH_2- and COOH-terminal interaction inhibited binding and activation by transcriptional intermediary factor 2. We conclude that the androgen receptor NH_2- and COOH-terminal interaction reduces the dissociation rate of bound androgen, stabilizes the receptor, and inhibits p160 coactivator recruitment by activation function 2.

The androgen receptor (AR)[1] is a member of the steroid receptor family of nuclear receptors that act as ligand-dependent transcriptional regulators. The AR shares with other steroid receptors an overall structural arrangement that includes a COOH-terminal ligand binding domain, central DNA binding region, and a less well conserved NH_2-terminal region (Fig. 1). Within these domains are two major transactivation regions, activation function 1 in the NH_2-terminal region and activation function 2 (AF2) in the ligand binding domain. The NH_2-terminal activation function 1 region, although not well defined, requires androgen binding for transcriptional activity and appears to be critical for AR-mediated gene activation. The AF2 region in the ligand binding domain forms a putative hydrophobic binding site for the L*XX*LL motifs of p160 coactivators (1–6), as recently revealed in the crystal structure of the AR ligand binding domain (7, 8). The p160 group of transcriptional coregulators includes steroid receptor coactivator 1 (SRC1), transcriptional intermediary factor 2 (TIF2, SRC2), and the SRC3/TRAM1/AIB1/pCIP/ACTR/RAC3 group of activators (9, 10), which are associated with histone acetyltransferase activity and can recruit CREB-binding protein, pCAF, and other coactivators required for chromatin modification (11).

The contribution of the AF2 region to AR-mediated transcriptional activity is unclear. Androgen-dependent transcriptional activity of an AR DNA and ligand binding domain fragment (AR-(507–919)) was only observed in cells that overexpressed TIF2 or SRC1 (12), which suggests that the AR AF2 inefficiently recruits p160 coactivators. We also showed recently that AF2 in the AR ligand binding domain can function in addition as a binding site for the AR NH_2-terminal region. Mutagenesis studies indicated that the androgen-induced interaction between the AR NH_2- and COOH-terminal (N/C) domains is mediated by two L*XX*LL-related sequences in the AR NH_2-terminal region (see Fig. 1). These are FQNLF (F*XX*LF motif) at residues 23–27 and WHTLF (W*XX*LF motif) at residues 433–437 (13). In the presence of androgen, the F*XX*LF motif interacts with the AR AF2 in the ligand binding domain, whereas interaction of the W*XX*LF motif remains to be characterized (12, 13). Most importantly, the N/C interaction is selectively induced by ligands that have AR agonist activity *in vivo*, such as the high affinity, biologically active androgens testosterone and dihydrotestosterone and the lower affinity anabolic steroids. In striking contrast, the N/C interaction is not induced by ligands that bind the AR and cause its nuclear transport but fail to induce AR-mediated gene activation *in vivo* (14). The N/C interaction therefore appears to be critical for AR function *in vivo* as further evidenced by the association of the androgen insensitivity syndrome with single amino acid mutations that disrupt the N/C interaction (12, 15).

In the present study we made use of two strategies to test the effects of the N/C interaction on AR function. We investigated to what extent the AR AF2 recruits p160 coactivators in the presence and absence of the N/C interaction in wild-type and mutant AR. Second, we took advantage of the observation that the agonist-induced N/C interaction (16), which was also reported for estrogen receptor α (17) and the progesterone recep-

* This work was supported by NICHD, National Institutes of Health (NIH) Public Health Service Grant HD16910, by cooperative agreement U54-HD35041 as part of the Specialized Cooperative Centers Program in Reproductive Research of National Institutes of Health, and by the International Training and Research in Population and Health Program supported by the Fogarty International Center and NICHD, NIH. The costs of publication of this article were defrayed in part by the payment of page charges. This article must therefore be hereby marked "*advertisement*" in accordance with 18 U.S.C. Section 1734 solely to indicate this fact.

‡ To whom correspondence should be addressed: CB# 7500, Rm. 374, Medical Sciences Research Bldg., University of North Carolina, Chapel Hill, NC 27599. Tel.: 919-966-5168; Fax: 919-966-2203; E-mail: emw@med.unc.edu.

[1] The abbreviations used are: AR, androgen receptor; TIF2, transcriptional intermediary factor 2; AF2, activation function 2; SRC1, steroid receptor coactivator 1; N/C, NH_2- and COOH-terminal; GR, glucocorticoid receptor; DMEM, Dulbecco's modified Eagle medium; R1881, methyltrienolone; $t_{1/2}$, half-time; CREB, cAMP-response element-binding protein; PCR, polymerase chain reaction; DHT, dihydrotestosterone; MEM, minimum essential medium.

tor (18), does not occur in the glucocorticoid receptor (GR) (19). Chimeras were created in which the three L*XX*LL motif region of TIF-2 was fused to the NH_2-terminal region of AR and GR. TIF-2 was shown previously to increase the transcriptional activity of nuclear receptors through interaction of its L*XX*LL motifs with the AF2 region of nuclear receptors (3, 5, 12, 13, 20). The effects of an imposed N/C interaction in the TIF2(L*XX*LL)$_3$ glucocorticoid receptor chimeras were determined by measuring rates of ligand dissociation and protein degradation. The results indicate that two functional effects of the N/C interaction are agonist-induced receptor stabilization and inhibition of p160 coactivator recruitment.

EXPERIMENTAL PROCEDURES

Preparation of AR and GR Expression Vectors—pCMVhARL26A/F27A (AR-F*XX*AA) is the full-length AR expression vector with the coding region for ^{23}FQNLF^{27} changed to ^{23}FQNAA^{27}. ARL26A/F27A/L436A/F437A (AR-F*XX*AA/W*XX*AA) has in addition ^{433}WHTLF^{437} changed to ^{433}WHTAA^{437} as described previously (13). AR-(507–919) codes for the AR DNA binding domain and ligand binding domain residues 507–919 (21). AR-E897K, AR-I898T, and AR-V716R have single amino acid mutations in the AF2 region and were previously described (12). pCMVhAR-W433A/L436A/F437A (AR-A*XX*AA) was constructed by digesting glutathione *S*-transferase-AR-(334–566)-W433A/L436A/F437A with *Bst*EII/*Kpn*I, and the fragment was subcloned in similarly digested pCMVhAR. AR-(1–503)-L26A/F27A (AR-(1–503)-F*XX*AA), AR-(1–503)-W433A/L436A/F437A (AR-(1–503)-A*XX*AA), and AR-(1–503)-L26A/F27A/W433A/L436A/F437A (AR-(1–503)-F*XX*AA/A-*XX*AA) were created by digesting AR-F*XX*AA, AR-A*XX*AA, and AR-F*XX*AA/A*XX*AA, respectively, with *Kpn*I/*Bam*HI and religating the vectors. pCMVhARΔ142–337L26A/F27A (ARΔ142–337F*XX*AA) was created by double PCR mutagenesis by amplifying AR-F*XX*AA (13), digesting with *Bgl*II/*Kpn*I, and subcloning into pCMVhARΔ142–337 digested with the same enzymes. GALAR-(624–919) and GALGR-(486–777) coding for fusion proteins of the GAL4 DNA binding domain and the AR and GR ligand binding domains were previously described (12). The GAL4 DNA binding domain-progesterone receptor fusion protein GAL-progesterone receptor 636–933 was prepared by PCR-amplifying the coding region for residues 636–933 in human progesterone receptor B and subcloning the fragment into pGAL0 (16).

TIF2(L*XX*LL)$_3$AR-(172–919) and TIF2(L*XX*AA)$_3$AR-(172–919) were constructed by PCR-amplifying the 627–780 amino acid region of pSG5TIF2 and pSG5TIF2 m123, where the latter has the 3 L*XX*LL motifs of TIF2 mutated to L*XX*AA (3, 20). The fragments were digested with *Bgl*II/*Afl*II and subcloned into pCMVhAR digested with the same enzymes. This removes the first 171 NH_2-terminal amino acid residues from human AR and places the TIF2 sequences NH_2-terminal and in-frame. TIF2(L*XX*LL)$_3$AR-(172–780)-A*XX*AA was constructed by PCR-amplifying the same 627–780-amino acid region of pSG5TIF2. The fragment was digested as above and subcloned in AR-A*XX*AA, which has the ^{433}W*XX*LF^{437} motif mutated to ^{433}A*XX*AA^{437}. SRC1(L*XX*LL)$_3$ AR-(172–919) was constructed by PCR-amplifying the 611–780-amino acid region of SRC1a (22, 23), digesting with *Bgl*II/*Afl*II, and subcloning into pCMVhAR digested with the same enzymes, which removes the NH_2-terminal 171 residues of AR. AIB1(L*XX*LL)$_3$AR-(172–919) was constructed by PCR-amplifying the 600–770-amino acid region of AIB1 (24), digesting with *Bgl*II/*Afl*II, and subcloning into pCMVhAR digested with the same enzymes, which removes the first 171 human AR residues.

TIF2(L*XX*LL)$_3$GR-(132–777) and TIF2(L*XX*AA)$_3$GR-(132–777) were constructed by PCR-amplifying the 627–780 residue region of pSG5TIF2 or pSG5TIF2 m123 as above. The fragments were digested with *Kpn*I/*Sal*I and subcloned into pCMVhGR digested with the same enzymes. This removes 131 NH_2-terminal amino acid residues of human GR. TIF2(L*XX*LL)$_3$GR and TIF2(L*XX*AA)$_3$GR were constructed by PCR-amplifying the 2–132-amino acid region of pCMVhGR and subcloning the *Sal*I fragment into TIF2(L*XX*LL)$_3$GR-(132–777) and TIF2(L*XX*AA)$_3$GR-(132–777). This reinserts the NH_2-terminal 2–132 residues of GR. The sequence of all PCR-amplified regions was verified by automated DNA sequencing.

Transcriptional Assays—Cell lines and transfection methods were selected to optimize transcriptional activity (CV-1 or HeLa cells) or expression levels (COS cells). Among these different cell lines we did not observe qualitative differences in response. Monkey kidney CV1 cells were plated at 4.2×10^5 cells/6-cm dish in 5% bovine calf serum in Dulbecco's modified Eagle's medium (DMEM) containing 20 mM Hepes, pH 7.2, penicillin and streptomycin, and 2 mM L-glutamine in a 5% CO_2 incubator at 37 °C. The same day 0.1 μg/plate of pCMVhAR or pCMVhGR wild-type or mutant expression vectors and 5 μg/plate of mouse mammary tumor virus luciferase reporter vector were separated into aliquots for 6 plates/14-ml Falcon tubes and stored at −50 °C overnight. The next day 0.21 ml of $H_2$0/plate and 30 μl/plate of freshly prepared 2 M $CaCl_2$ were added to the DNAs followed by 0.24 ml 2× Hepes-buffered saline/plate (0.28 M NaCl, 1.5 mM Na_2HPO_4, 0.05 M Hepes, pH 7.2) while vortexing. After 30 min at room temperature to allow for calcium phosphate precipitation, the mixture was briefly vortexed, and 0.475 ml was added to each plate containing 4 ml of 5% bovine calf serum in DMEM. The cells were incubated for 4 h, the media were aspirated, and the cells were incubated for 3 min with 1.5 ml of 15% glycerol in DMEM containing 5% bovine calf serum followed by a 4-ml phosphate-buffered saline wash. Cells were placed in 4 ml of serum-free, phenol red-free DMEM with and without hormones and incubated overnight. The following day, serum-free media with and without hormone were replaced, and the cells were incubated 24 h. The next day cells were washed with 4 ml of phosphate-buffered saline and aspirated dry, 0.5 ml of lysis buffer (25 mM Trizma (Tris base) phosphate, pH 7.8, 2 mM EDTA, 1% Triton X-100) was added, and 0.1 ml analyzed for luciferase activity using a Monolight luminometer.

To determine transcriptional activity induced by the GAL4 DNA binding domain and receptor ligand binding domain fusion proteins, HeLa cells plated at 3×10^5 cells/6-cm dish in minimal essential medium (MEM) containing 10% fetal bovine serum, penicillin and streptomycin, and 2 mM L-glutamine in a 5% CO_2 incubator at 37 °C. Cells were transfected with 0.25 μg each/plate of the GAL4-AR ligand binding domain, GAL4-GR ligand binding domain, and GAL4-progesterone receptor ligand binding domain vectors described above, pSG5TIF2 and G5E1b-luciferase reporter, which contain 5 tandem GAL4 binding sites. The day after plating, medium was replaced with fresh MEM containing 10% fetal bovine serum. DNA was combined with 0.15 ml of EC buffer/plate (Qiagen) and 4 μl of enhancer/plate, vortexed, and incubated for 5 min at room temperature. Effectene reagent (Qiagen, 4 μl/plate) was added, vortexed for 10 s, and incubated for 10 min. MEM containing 10% serum was added (1 ml/plate) and mixed, and 1 ml of the DNA solution was added to each plate. After incubation overnight at 37 °C, cells were washed with 4 ml of phosphate-buffered saline, and 4 ml of serum-free, phenol red-free MEM with and without hormones was added per plate as indicated. The next day cells were washed with phosphate-buffered saline and harvested in 0.5 ml of lysis buffer described above and analyzed for luciferase activity.

Ligand Dissociation Rate Studies—Monkey kidney COS cells were plated at 0.4×10^6 cells/well in 6-well plates in 3 ml of 10% bovine calf serum in DMEM containing 20 mM Hepes, pH 7.2, penicillin and streptomycin, and 2 mM L-glutamine in a 5% CO_2 incubator at 37 °C. Cells were transfected with 2 μg/well pCMVhAR or pCMVhGR wild-type or mutant DNA using 0.95 ml/well of 1.08× TBS (TBS: 0.14 M NaCl, 3 mM KCl, 1 mM $CaCl_2$, 0.05 mM $MgCl_2$, 0.9 mM NaH_2PO_4, and 25 mM Tris, pH 7.4) and 0.11 ml/well of 500 mg/ml DEAE-dextran. Media were aspirated, 1 ml of DNA solution was added, and the cells were incubated for 30 min at 37 °C. Media were aspirated, and 3 ml of a chloroquine-medium solution (1 ml of 5 mg/ml chloroquine/100 ml DMEM containing 10% bovine calf serum) was added per well. Cells were incubated for 3 h at 37 °C. Media were aspirated, and the cells were incubated for 4 min at room temperature with 1 ml of 15% glycerol in DMEM containing 10% bovine calf serum. The glycerol medium was aspirated, and the cells were washed with 3 ml of TBS. Cells were placed with 3 ml of DMEM containing 10% bovine calf serum at 37 °C. After 48 h, the medium was aspirated, and 0.6 ml of labeling medium was added containing 5 nM [^{3}H]R1881 (methyltrienolone, 17α-[*methyl*-^{3}H]R1881, 70–87 Ci/mmol, PerkinElmer Life Sciences) for AR or 8 nM [^{3}H]dexamethasone ([1,2,4,6,7-^{3}H]dexamethasone, 84 Ci/mmol, Amersham Pharmacia Biotech) for GR and incubated for 2 h at 37 °C. Sufficient wells were labeled to allow multiple time points for specific and nonspecific binding, the latter determined by incubating in the presence of a 100-fold excess of unlabeled hormone. Dissociation rate studies performed at 35 °C were initiated by adding to the labeling media a 10,000-fold molar excess of unlabeled hormone (0.1 ml/well). Cells were carefully washed once with 3 ml of phosphate-buffered saline at different time intervals and harvested in 0.5 ml of 10 mM Tris, pH 6.8, 2% SDS and 10% glycerol, and radioactivity was determined by scintillation counting.

Immunoblots—Relative expression levels and stability of wild-type and mutant AR and GR were determined by immunoblot analysis. COS cells were plated in DMEM containing 10% bovine calf serum at 1.6 ×

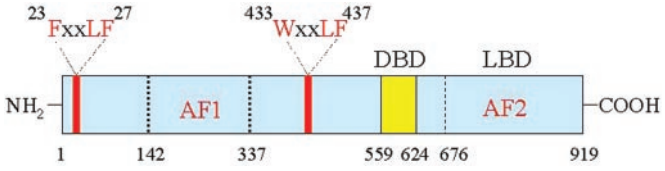

FIG. 1. **Schematic diagram of the human AR with 919 amino acid residues comprised of the F*XX*LF motif (^{23}FQNLF^{27}), W*XX*LF motif (^{433}WHTLF^{437}), AF1 (residues 142–337), AF2 in the ligand binding domain, the DNA binding domain (*DBD*, residues 559–624), and the ligand binding domain (*LBD*, residues 676–919).**

10^6 cells/10-cm dish and the next day incubated for 3 h at 37 °C with 3 ml/plate containing 10 μg of expression vector DNA, 2.85 ml of 1.08× TBS, and 0.33 ml of 5 mg/ml DEAE-dextran solution. The DNA mix was aspirated, and the cells were treated with 3 ml of chloroquine medium (see paragraph above) per well. Cells were incubated for 3 h at 37 °C and then with 3 ml of glycerol media as described above, washed once with 8 ml of TBS, and incubated in DMEM containing 10% bovine calf serum at 37 °C. The next day cells were placed in phenol red-free, serum-free media with or without 0.5 μM DHT or 1 μM dexamethasone and incubated for 24 h. Cells were washed in 8 ml of cold phosphate-buffered saline and harvested in 1 ml of phosphate-buffered saline, centrifuged, and solubilized in 0.2 ml of 50 mM Tris, pH 7.5, 0.15 M NaCl, 0.5% Nonidet P-40, 50 mM NaF, 1 mM $NaVO_3$, 1 mM dithiothreitol, 1 mM phenylmethylsulfonyl fluoride, and Sigma protease inhibitor mixture for mammalian cells (P8340). Protein concentrations were determined using the Bio-Rad protein assay with bovine serum albumin as standard. Extracts were separated on 10% acrylamide gels containing SDS and analyzed by immunoblot for GR using rabbit polyclonal anti-human GR antibody (Affinity BioReagents) at 1:2500 dilution. AR was detected on immunoblots using mouse monoclonal AR antibody F39.4.1 raised against human AR peptide residues 302–321 (25) (Biogenex, San Ramon, CA) and used for immunoblots at 1:10,000 dilution or rabbit polyclonal antibody C19 raised against human AR peptide residues 901–919 (Santa Cruz Biotechnology, Inc., Santa Cruz, CA) and used at 0.2 μg/ml. Secondary antibody goat-anti-mouse IgG or goat anti-rabbit IgG conjugated to horseradish peroxidase (Amersham Pharmacia Biotech) were used for detection by enhanced chemiluminescence (Pierce).

Degradation Rate Studies—Degradation rates of AR and mutants were determined at 35 °C in the presence of 5 nM DHT by pulse-chase [^{35}S]methionine labeling in transiently transfected COS cells as previously described (19). The full-length AR mutants analyzed included AR-E897K, AR-I898T, and AR-V716R, which are mutations in the AF2 region of the ligand binding domain (12).

RESULTS

Specificity of the NH_2-terminal Motif in the N/C Interaction—Mutations in AR NH_2-terminal sequences ^{23}FQNLF^{27} (F*XX*LF motif) and ^{433}WHTLF^{437} (W*XX*LF motif) (Fig. 1) disrupt the N/C interaction, which results in an increase in the dissociation rate of bound androgen. As previously reported (13), the dissociation half-time ($t_{1/2}$) of the radiolabeled synthetic androgen [^{3}H]R1881 measured at 35 °C was 158 min for full-length AR and decreased to 89 min by mutating F*XX*LF to F*XX*AA. Mutation of W*XX*LF to W*XX*AA by itself had no effect on the androgen dissociation rate (13), whereas mutating both F*XX*LF and W*XX*LF to F*XX*AA and W*XX*AA decreased the $t_{1/2}$ to 43 min (Fig. 2*A* and Fig. 3). Mutations in both NH_2-terminal motifs resulted in a ligand dissociation rate equal to that observed for AR-(507–919) ($t_{1/2}$ 44 min), a mutant that lacks the entire NH_2-terminal region (Fig. 2*B* and Fig. 3).

We used the same strategy to test for the relative effectiveness of L*XX*LL motifs of TIF2 to interact with AF2 in the AR ligand binding domain. TIF2-AR chimeras were created in which AR amino acid residues 1–171 containing the F*XX*LF motif were replaced by TIF2 residues 627–780 that include the 3 L*XX*LL motif region (3). TIF2(L*XX*LL)$_3$AR had a dissociation half-time for [^{3}H]R1881 of 97 min (Fig. 2*B*, TIFLXL3 and Fig. 3), which suggested that the interaction of the 3 TIF2 L*XX*LL with the AR ligand binding domain is weaker compared with that of the single AR F*XX*LF motif. Specificity of the interaction in TIF2(L*XX*LL)$_3$AR was assessed in two control experiments. Mutation of the 3 L*XX*LL motifs in TIF2 to L*XX*AA (Fig. 2*B*, TIFLXA3AR and Fig. 3) and of the second N/C AR interaction domain W*XX*LF to A*XX*AA similarly decreased the dissociation half-time of TIF2(L*XX*LL)$_3$AR from 97 min to ~60 min, which was ~15 min longer than the $t_{1/2}$ of 44 min for AR-(507–919) (Fig. 2*B* and Fig. 3). The results support a limited interaction between the three L*XX*LL motifs of TIF2 and the AR ligand binding domain compared with that observed with the single AR NH_2-terminal F*XX*LF sequence.

The relevance of ligand dissociation studies with the TIF2/AR chimeras was tested further by creating TIF2/GR chimeras. We chose the GR because we had found previously that deletion of the GR NH_2-terminal region (residues 1–398) did not change the rapid dissociation rate of [^{3}H]dexamethasone (19), supporting the absence of an N/C interaction in GR. Replacing NH_2-terminal GR amino acid residues 1–131 with the same (L*XX*LL)$_3$-containing region of TIF2 dramatically slowed the dissociation half-time of [^{3}H]dexamethasone from GR from 31 to 168 min (Fig. 2*C*, TIFLXL3GR and Fig. 3). The effectiveness of the L*XX*LL motifs to slow ligand dissociation from GR in the TIF2-GR chimera contrasted the relative inability of this region to slow the dissociation rate of [^{3}H]R1881 from TIF2(L*XX*LL)$_3$/AR-(172–919)/A*XX*AA ($t_{1/2}$ 64 min) when compared with AR-F*XX*AA/W*XX*AA ($t_{1/2}$ 43 min) and AR-(507–919) ($t_{1/2}$ 44 min). The results suggest a much more effective interaction of the p160 coactivator L*XX*LL motifs with the GR ligand binding domain compared with that with the AR ligand binding domain. Remarkably, with the NH_2-terminal insertion of the TIF2 L*XX*LL motif region, the dissociation half-time of [^{3}H]dexamethasone from GR decreased to the same slow dissociation half-time as observed for [^{3}H]R1881 from AR caused by the N/C interaction with the naturally occurring F*XX*LF motif. When the TIF2 L*XX*LL motifs were mutated in the TIF2-GR chimera to TIF2(L*XX*AA)$_3$GR-(132–777), the ligand dissociation half-time was indistinguishable from that of wild-type GR ($t_{1/2}$ 28 min, Fig. 2*C*, TIFLXA3GR and Fig. 3). These results demonstrate that it was the L*XX*LL motifs in the TIF2 fragment that simulated an N/C interaction in GR, causing a dramatic reduction in dissociation half-time of [^{3}H]dexamethasone. The same dependence on the L*XX*LL motifs was obtained using fusion proteins with the TIF2 (L*XX*LL)$_3$ region expressed at the NH_2 terminus of full-length GR (Fig. 3).

We compared the relative effects of the (L*XX*LL)$_3$ region of TIF2 with those of two other members of the p160 coactivator family. Replacement of the NH_2-terminal 171 amino acid residues of AR with the (L*XX*LL)$_3$ motif regions of SRC1 or AIB1 indicated that these regions of SRC1 ($t_{1/2}$ 58 min) and AIB1 ($t_{1/2}$ 51 min) in the chimeras each slowed the ligand dissociation rate to less of an extent than the same region of TIF2 ($t_{1/2}$ 97 min) and considerably less than the reduction induced by AR F*XX*LF ($t_{1/2}$ 158 min, Fig. 3). Taken together, the data of Figs. 1–3 indicate that none of the L*XX*LL motifs in the 3 p160 coactivators tested was as effective as the single F*XX*LF motif in AR in slowing the dissociation rate of bound androgen. The results suggest that the AF2 region of AR interacts preferentially with the F*XX*LF motif. The results raised the question of whether these L*XX*LL motifs of the p160 coactivators can compete for the AR interdomain N/C interaction and activate the AR through the AF2 region of the ligand binding domain. We tested this in cotransfection assays with increasing amounts of TIF2 DNA.

Influence of the N/C Interaction on TIF2 Activation of AF2—The ability of the N/C interaction to influence AR activation by

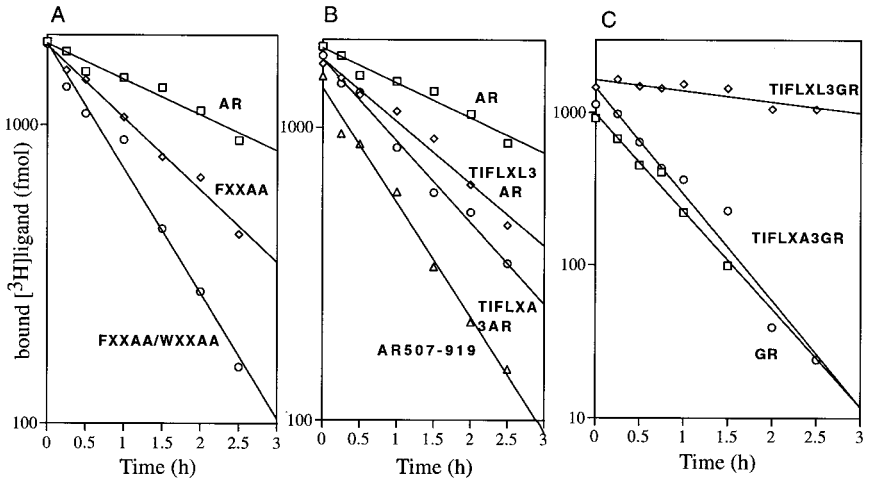

FIG. 2. **Dissociation rate studies of wild-type and mutant AR and GR.** Dissociation half-times of bound [^{3}H]R1881 from AR and [^{3}H]dexamethasone from GR were determined in COS cells transfected as described under "Experimental Procedures." In *A* the full-length pCMVhAR (AR-(1–919) (*AR*)) and mutants included ^{23}FQNLF^{27} changed to ^{23}FQNAA^{27} (F*XX*AA), and this mutation combined with ^{433}WHTLF^{437} changed to ^{433}WHTAA^{437} (F*XX*AA/W*XX*AA). In *B* the AR mutants included AR-(507–919), substitution of the AR NH_2-terminal 171-amino acid residues with TIF2 residues 627–780 containing the 3 L*XX*LL motif region (TIF2(L*XX*LL)$_3$AR-(172–919), TIFLXL3AR), and the same vector except the last two leucines of each L*XX*LL motif changed to alanine (TIF2(L*XX*AA)$_3$AR-(172–919), TIFLXA3AR). In *C* the NH_2-terminal 131-amino acid residues of GR were replaced by TIF2 residues 627–780 containing the 3 L*XX*LL motif region (TIF2(L*XX*LL)$_3$GR-(132–777), TIFLXL3GR) and the same vector except with the last two leucines of each L*XX*LL motif changed to alanine (TIF2(L*XX*AA)$_3$GR-(132–777), TIFLXA3GR). Dissociation half-times are summarized in Fig. 3.

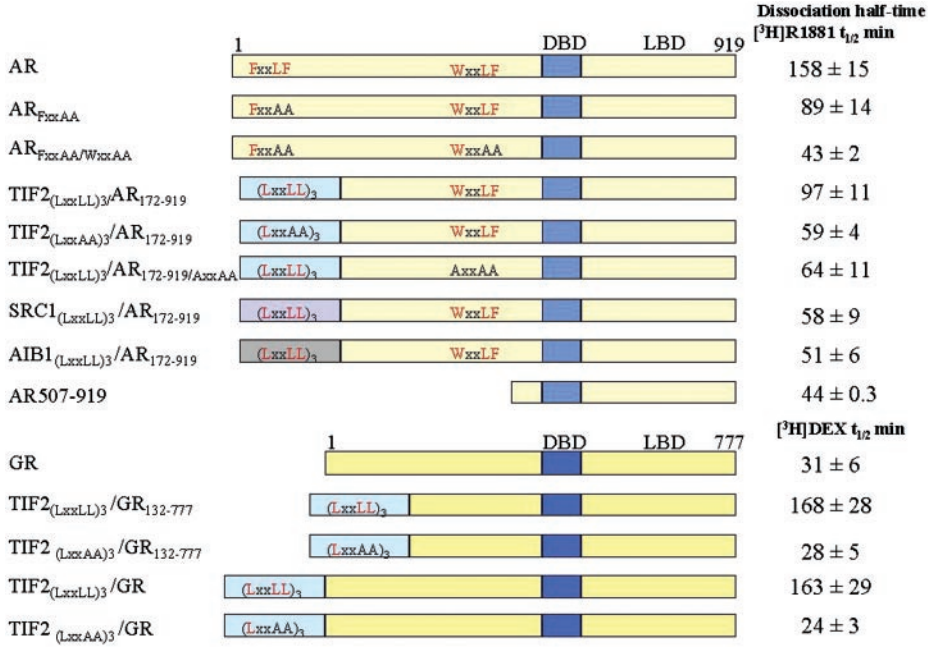

FIG. 3. **Schematic diagram of AR and GR mutants and summary of dissociation half-times.** Indicated schematically are mutants described under "Experimental Procedures" and the dissociation half-times (in min) ± S.D. determined from three independent experiments at 35 °C. Also indicated are the DNA binding domain (*DBD*) and ligand binding domain (*LBD*). *DEX*, dexamethasone.

the p160 coactivators was assessed by measuring transcriptional activation of AR and AR mutants and, in control experiments, of the TIF2/GR chimeras that mimicked the N/C interaction of the AR. In initial studies, we compared the intrinsic AF2 activities of the ligand binding domains of AR, the progesterone receptor, and GR in GAL4-DNA binding domain fusion proteins and their relative activation by TIF2 in the absence of the activation function 1 NH_2-terminal region. Intrinsic androgen-dependent AR AF2 activity was not detected as previously reported (12), whereas GAL4-ligand binding domain fusion proteins of progesterone receptor and GR-mediated 6- and 33-fold induction, respectively, in the presence of hormone (Fig. 4). TIF2 overexpression resulted in only a 23-fold activation of GAL-AR ligand binding domain compared with the 197- and 193-fold induction of GAL-progesterone receptor ligand binding domain and GALGR-ligand binding domain, respectively, in the presence of hormone (Fig. 4). The results indicate that compared with the progesterone receptor and GR ligand binding domain, the AR ligand binding domain has inherently weak AF2 activity that could be overcome to some extent by TIF2 overexpression.

The high transcriptional activity of the AR NH_2-terminal activation function 1 region (amino acid residues 142–337, Fig. 1) (26) makes it difficult to measure AF2 activity in the presence of activation function 1. A deletion mutant (ARΔ142–337) was therefore used in which the NH_2-terminal transactivation domain residues 142–337 were deleted, but the N/C interaction remained intact, as indicated by two hybrid assays (12) and a ligand dissociation rate equivalent to wild-type AR (19). Increasing the amount of transfected pSG5TIF2 expression vector DNA from 0.2 to 5 μg was relatively ineffective in activating ARΔ142–337, with only a 12-

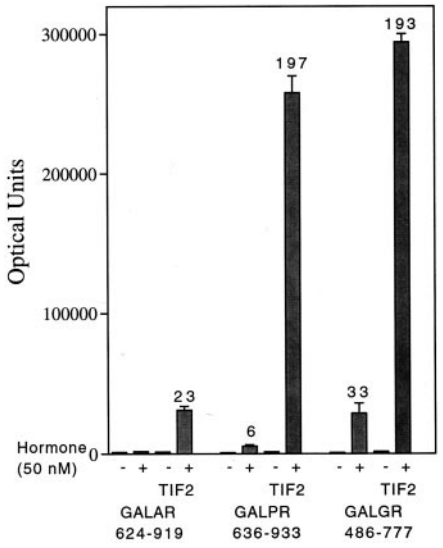

FIG. 4. **Intrinsic AF2 activity of the AR, progesterone receptor, and GR ligand binding domains.** DNA (0.25 μg/plate) for the GAL4 DNA binding domain and ligand binding domains for AR (GALAR-(624–919)), progesterone receptor (GALPR-(636–933)) and GR (GALGR-(486–777)) were transfected into HeLa cells with or without 0.25 μg of pSG5TIF2 (TIF2) and 0.25 μg of G5E1b-luciferase reporter using Effectene as described under "Experimental Procedures." Cells were incubated in the absence and presence of 50 nM DHT for AR, 50 nM R5020 for progesterone receptor, and 50 nM dexamethasone for GR. Luciferase activity was determined as described under "Experimental Procedures," and the fold induction relative to the activity was determined in the absence of hormone is shown above the *bars*.

fold activation detected with 5 μg TIF2 DNA (Fig. 5*A*). In striking contrast, with a construct in which the N/C interaction was weakened by changing the ^{23}F*XX*LF^{27} motif to ^{23}F*XX*AA^{27} (ARΔ142–337F*XX*AA, Fig. 5*A*), TIF2 was about 100 times more effective in increasing AR-mediated transactivation based on the amount of transfected TIF2 DNA. A similar activation of 12–13-fold was observed using 5 μg of TIF2 with ARΔ142–337 or 0.05 μg of TIF2 with ARΔ142–337F*XX*AA. However, TIF2 activation of ARΔ142–337F*XX*AA was less than that observed when the entire NH_2-terminal region was deleted (Fig. 5*A*). The weaker activation by TIF2 of ARΔ142–337F*XX*AA compared with that with AR-(507–919) likely resulted from the presence of the ^{433}WHTLF^{437} sequence in ARΔ142–337F*XX*AA, as this W*XX*LF motif contributes to the N/C interaction (13) and therefore may partially inhibit TIF2 recruitment by AF2.

We also tested transcriptional coactivation of AF2 using a TIF2 mutant in which all three L*XX*LL motifs were changed to L*XX*AA. TIF2(L*XX*AA)$_3$ did not coactivate with ARΔ142–337, ARΔ142–337F*XX*AA, or AR-(507–919) above the low intrinsic levels observed with the mutant AR alone (Fig. 5*B*). Especially striking was the decrease in transcriptional activation with ARΔ142–337F*XX*AA and AR-(507–919) from 179- and 290-fold with TIF2 to near background levels with the TIF2(L*XX*AA)$_3$ mutant. The results of Figs. 5, *A* and *B*, suggest that the androgen-induced AR N/C interaction mediated by the F*XX*LF and W*XX*LF motifs inhibits p160 coactivator interaction with AF2 in the ligand binding domain. Mutations in the F*XX*LF region were required to significantly overcome the androgen-induced inhibition imposed by the N/C interaction on p160 coactivator recruitment by AF2.

Similar dose-response studies were performed using TIF2-GR chimeras. Introducing the putative N/C interaction in TIF2-(L*XX*LL)$_3$GR-(132–777) resulted in a reduced response to TIF2 activation compared with that observed with the TIF2(L*XX*AA)$_3$GR-(132–777) mutant (Fig. 5*C*). A 10-fold higher amount of TIF2 was required to activate TIF2(L*XX*LL)$_3$GR-(132–777) (0.5 μg of TIF2, 160-fold) above background levels compared with 0.05 μg, the lowest level of TIF2 tested with the L*XX*AA mutant (142-fold, Fig. 5*C*). Thus, in agreement with results with AR, the N/C interaction imposed in GR by insertion of the NH_2-terminal L*XX*LL motifs attenuated activation of the receptor by TIF2. It is nevertheless noteworthy that increased TIF2 expression (5 μg of pSG5TIF2 DNA) was effective in overcoming the inhibition created by the artificially induced N/C interaction in GR, suggesting that a coregulatory protein with a binding region of similar or greater affinity for AF2 can compete more efficiently for the N/C interaction if it is expressed at sufficiently high levels.

Effect of the FXXLF, WXXLF, and LXXLL Motifs on Receptor Stabilization—An unusual property of the AR is its dramatic stabilization by agonist binding (27), which previous data suggested is mediated by the N/C interaction (15). In contrast, most steroid receptors including the estrogen receptor α (28, 29), thyroid hormone receptor (30), GR (31), and progesterone receptor (32) undergo agonist-induced decreases in receptor levels. To further investigate the contribution of the N/C interaction to androgen-induced AR stabilization, we determined the effects of mutations in the NH_2-terminal F*XX*LF and W*XX*LF interaction motifs on AR levels by immunoblot analysis. The addition of 0.5 μM DHT to the growth media resulted in a dramatic increase in AR protein (Fig. 6*A*, *lanes 2* and 3), indicating androgen-induced receptor stabilization. In contrast, the F*XX*AA as well as the F*XX*AA/A*XX*AA double mutant AR proteins were detected at similar levels in the absence and presence of DHT (Fig. 6A, *lanes 4–7*). We also noted that in the absence of androgen there was a reproducible increase in the levels of these AR mutants relative to wild-type AR. The results support a role of the F*XX*LF and W*XX*LF-mediated N/C interaction in ligand-induced AR stabilization.

We further investigated the influence of the F*XX*LF and W*XX*LF-mediated N/C interaction on AR stabilization by coexpression of the COOH-terminal fragment AR-(507–919) that contains the DNA and ligand binding domains together with wild-type AR NH_2-terminal fragment AR-(1–503) and AR-(1–503) fragments containing the F*XX*AA and A*XX*AA mutations. Coexpression of AR-(507–919) with wild-type AR-(1–503) resulted in a modest increase in AR-(507–919) levels assayed in the presence of 0.5 μM DHT (Fig. 6*B*, *lanes 1* and *2*). Mutations in the F*XX*LF, W*XX*LF, or both motifs in AR-(1–503), which decrease the N/C interaction between AR-(1–503) and AR-(507–919), result in reduced protein levels of AR-(507–919), although surprisingly, no major changes in protein levels of the AR-(1–503) fragments were observed (Fig. 6*B*). The data further support an NH_2-terminal F*XX*LF- and W*XX*LF-motif role in androgen-induced AR stabilization.

We made use of the TIF2-GR chimeras to substantiate the role of the N/C interaction in receptor stabilization. Full-length GR undergoes a striking agonist-induced decrease in receptor levels with the addition of 1 μM dexamethasone (Fig. 6*C*, *lanes 1* and 2). In contrast, the TIF2-GR chimera TIF2(L*XX*LL)$_3$GR-(132–777), which was shown above to dramatically slow the dissociation half-time of bound [^{3}H]dexamethasone (see Fig. 2*C* and Fig. 3), exhibited loss of dexamethasone-induced GR destabilization (Fig. 6*C*, *lanes 3* and *4*). When the last two leucine residues in each of the three L*XX*LL motifs were mutated to alanine in TIF2(L*XX*AA)$_3$GR-(132–777), which was shown above to reverse the ligand dissociation half-time to that of wild-type GR, degradation of the TIF2-GR chimera was indistinguishable from that of wild-type GR (Fig. 6*C*, *lanes 5* and *6*). Similar results were observed with the TIF2(L*XX*LL)$_3$GR chimeras in which the TIF2 fragment was expressed as a fusion

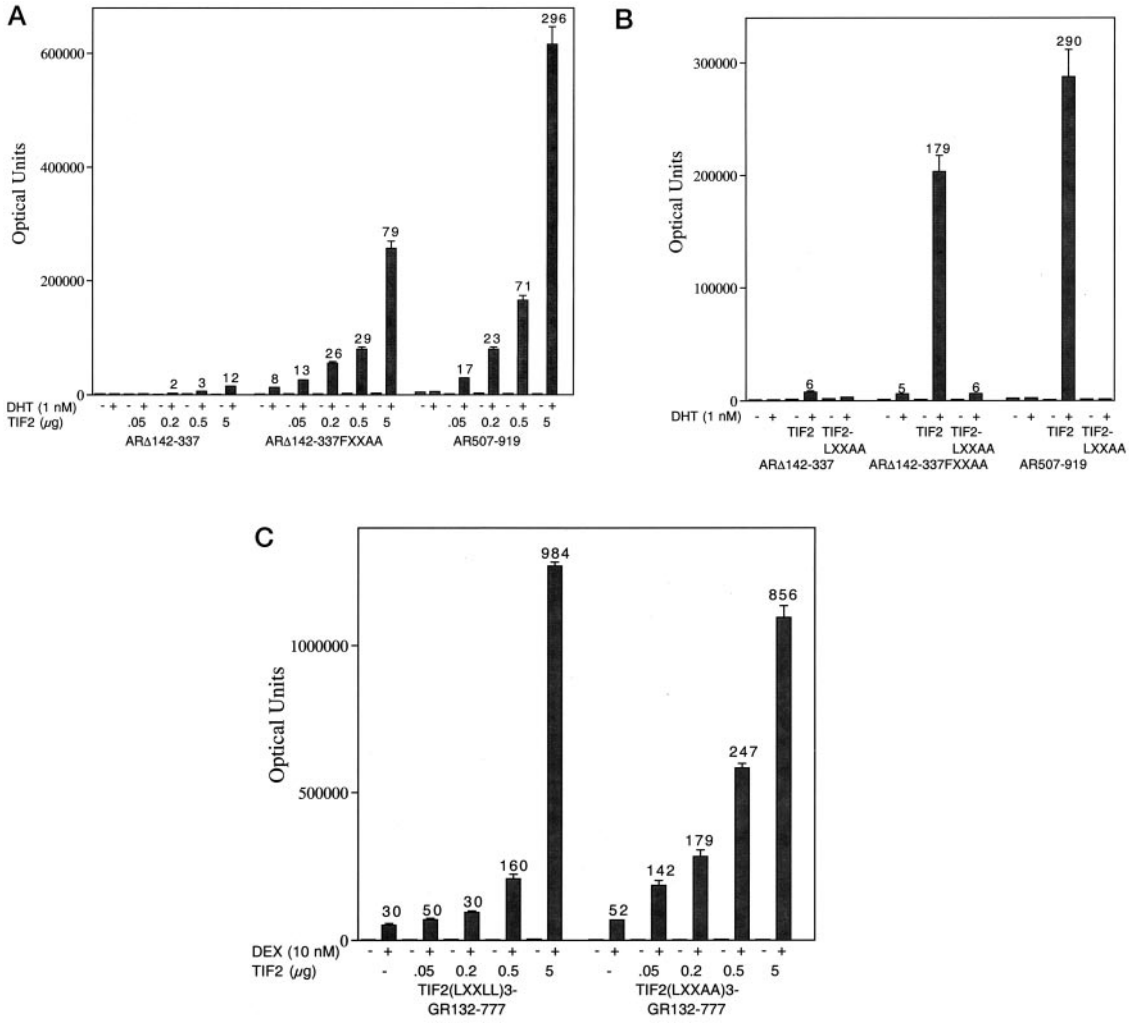

FIG. 5. **Effect of TIF2 expression on AR, GR, and TIF2-receptor chimera-mediated transactivation.** CV1 cells were transfected using calcium phosphate precipitation as described under "Experimental Procedures." with 5 μg of mouse mammary tumor virus luciferase reporter vector and 100 ng of AR or GR expression vector DNA. Shown are the luciferase light units, determined in the absence and presence of 1 nM DHT or 10 nM dexamethasone with fold induction indicated above the *bars*. In each part, the data are representative of at least three independent experiments. *A*, cells were transfected in the absence or with increasing amounts of pSG5TIF2 DNA from 0.05 to 5 μg together with ARΔ142–337 that lacks AF-1 residues 142–337, ARΔ142–337F*XX*AA in which the ^{23}F*XX*LF^{27} motif was mutated to F*XX*AA and activation function 1 deleted, and the DNA binding domain and ligand binding domain fragment AR-(507–919). *B*, CV1 cells were transfected using 0.1 μg of the AR mutants, 5 μg of mouse mammary tumor virus luciferase reporter without or with 5 μg of pSG5TIF2 (TIF2) or pSG5TIF2(L*XX*AA)$_3$ (TIF2-L*XX*AA). Cells were incubated in the absence and presence of 1 nM DHT, and luciferase activity and fold induction relative to the activity determined in the absence of DHT are indicated. *C*, TIF2(L*XX*LL)$_3$GR-(132–777) and TIF2(L*XX*AA)$_3$GR-(132–777) were expressed in CV1 cells in the absence and presence of increasing amounts of pSG5TIF2 DNA as indicated. Cells were incubated in the absence and presence of 10 nM dexamethasone.

protein with full-length GR, although the extent of stabilization was less pronounced (Fig. 6*C*, *lanes 7–10*). Taken together the results indicate that the agonist-induced N/C interaction increases the half-time of ligand dissociation and allows for agonist-induced receptor stabilization and the absence of agonist-induced destabilization that is characteristic of wild-type AR but not GR.

Degradation rates of AR and several AR mutants were determined using [^{35}S]methionine pulse-chase labeling. As summarized in Table I, mutation of the NH$_2$-terminal F*XX*LF and W*XX*LF motifs resulted in degradation rates intermediate between those of full-length AR and AR-(507–919), as determined in COS cells at 35 °C. Increased AR degradation in the presence of 5 nM DHT compared with that of wild-type AR was also observed for AR AF2 mutants E897K, I898T, and V716R. These mutations were shown previously to disrupt the N/C interaction (12). The results support a critical role for the N/C interaction in androgen-induced AR stabilization.

DISCUSSION

Several lines of evidence indicate that the agonist-induced N/C interaction between the L*XX*LL-like sequences ^{23}FQNLF^{27} and ^{433}WHTLF^{437} in the AR NH$_2$-terminal region and the AF2 region in the AR ligand binding domain is specific for AR and required for functional activity. The N/C interaction is critical to AR function, because AF2 mutations that disrupt the N/C interaction without affecting the equilibrium ligand binding affinity cause the androgen insensitivity syndrome, whereas mutations that disrupt p160 coactivator binding without affecting the N/C interaction have wild-type activity (12, 15). The N/C interaction slows ligand dissociation and increases AR stability yet interferes with p160 coactivator recruitment. Like the L*XX*LL motifs of p160 coactivators (1, 5), the AR F*XX*LF motif forms an amphipathic α-helix that interfaces within the hydrophobic groove of AF2.

Results of experiments with chimeric receptors indicate the AR N/C interaction has greater specificity and potency compared with the interaction of AF2 with the L*XX*LL motifs of

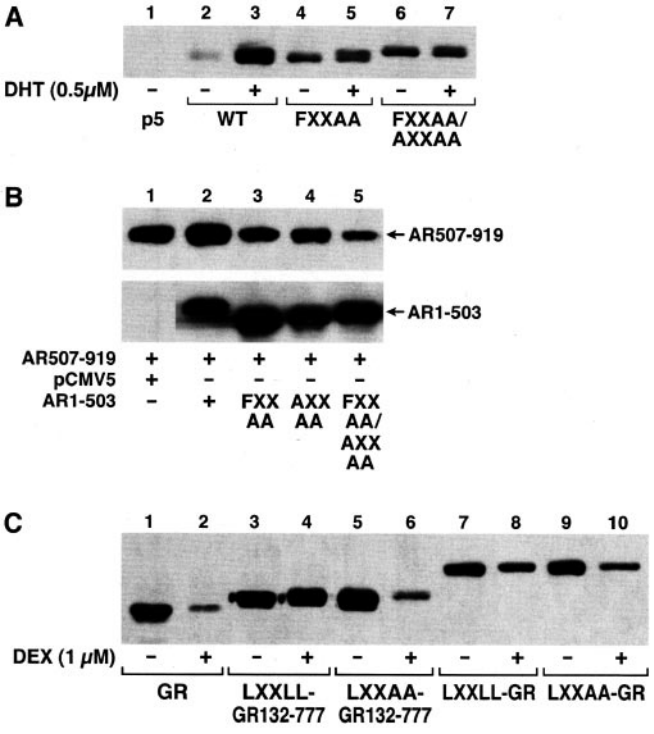

FIG. 6. **Immunoblot analysis of AR, GR, and mutants in the presence and absence of hormone.** Plasmids were expressed in COS cells in the presence and absence of hormone as indicated. Cell extracts (20 μg of protein) were analyzed on 10% acrylamide gels by immunoblot as described under "Experimental Procedures." *A*, full-length wild-type (*WT*) and mutant AR expression vectors included pCMV5 parent vector lacking AR sequence (p5, *lane 1*), wild-type pCMVhAR (WT, *lanes 2* and *3*), AR-F*XX*AA (*lanes 4* and *5*), and AR- F*XX*AA/A*XX*AA (*lanes 6* and *7*). Cells were incubated 24 h before harvest with or without 0.5 μM DHT as indicated. Immunoblots were developed using the C19 AR COOH-terminal antibody (Santa Cruz). *B*, AR-(507–919) (5 μg, AR DNA and ligand binding domain) was expressed in the presence of an equivalent molar amount of pCMV5 empty vector DNA (3 μg, *lane 1*) or 5 μg of AR-(1–503) coding for the AR NH_2-terminal region (*lane 2*), AR-(1–503)-F*XX*AA (*lane 3*), AR-(1–503)-A*XX*AA (*lane 4*), or AR-(1–503)-F*XX*AA/A*XX*AA (*lane 5*). Twenty-four h after transfection, cells were incubated with 0.5 μM DHT for another 24 h. The blot was probed with COOH-terminal AR rabbit polyclonal antibody C19 (Santa Cruz) at 0.2 μg/ml to detect AR-(507–919) and with mouse monoclonal antibody F39.4 (Biogenex) at 1:10,000 dilution to detect AR-(1–503). *C*, the effect of dexamethasone on GR and TIF2-GR chimera expression levels for full-length wild-type pCMVhGR (*GR*, *lanes 1–2*), $TIF2^{627–780}$(L*XX*LL)$_3$GR-(132–777) (*LXXLL-GR-(132–777)*, *lanes 3–4*), $TIF2^{627–780}$(L*XX*AA)$_3$GR-(132–777) (*LXXAA-GR-(132–777)*, *lanes 5–6*), $TIF2^{627–780}$(L*XX*LL)$_3$GR (*LXXLL-GR*, *lanes 7–8*), $TIF2^{627–780}$(L*XX*AA)$_3$GR (*LXXAA-GR*, *lanes 9–10*). Cells were incubated for 24 h before harvest in the absence (*odd-numbered lanes*) and presence (*even-numbered lanes*) of 1 μM dexamethasone (*DEX*). GR and the TIF2-GR chimeras were detected using rabbit polyclonal anti-human GR antibody (Affinity BioReagents).

p160 coactivators. In previous studies, AR/GR chimeras only slightly increased ligand dissociation half-times (19), suggesting that the F*XX*LF motif interacts less well with the GR AF2 than this region interacts with the TIF2-derived L*XX*LL motifs. In unpublished studies,[2] glutathione *S*-transferase affinity matrix assays showed that TIF2 L*XX*LL motif-containing fragments interact with the estrogen receptor α ligand binding domain, whereas the AR F*XX*LF fragment does not.

The AR AF2 region only weakly recruits p160 coactivators compared with the AF2 region of the progesterone or glucocorticoid receptor. This relatively weak interaction is further hindered by the N/C interaction. The hinge region of AR (residues 628–646) was reported to contribute to the low transcriptional activity of AR AF2 (34). However in our unpublished studies,[2] deletion of hinge residues 624–647 only minimally increased AR AF2 transcriptional activity of a GAL4 fusion protein with the AR ligand binding domain expressed in HeLa cells and resulted in a similar increase in the N/C interaction. The lower transcriptional activity of the AR AF2 region relative to other nuclear receptors more likely results from sequence divergence-induced structural differences and by the N/C interaction.

TABLE I

Degradation half-times determined in the presence of 5 nM DHT

Degradation half-times (in h) were determined in COS cells transiently transfected with the AR or the indicated AR mutants and analyzed at 35 °C in the presence of 5 nM DHT. Expressed AR was labeled with [^{35}S]methionine, and pulse-chase analysis was performed as described under "Experimental Procedures." Mutations are further defined under "Experimental Procedures." Shown are the means and error of at least three independent experiments.

	h
AR	12.0 ± 3.0
AR-(507–919)	2.4 ± 0.2
NH_2-terminal mutations	
F*XX*AA	5.6 ± 0.6
F*XX*AA/W*XX*AA	7.4 ± 0.8
AF2 mutations	
E897K	4.5 ± 1.8
I898T	6.2 ± 0.4
V716R	5.8 ± 0.2

One functional consequence of the agonist-induced AR N/C interaction may be to present a novel surface to attract AR-specific coactivators. A LIM domain, heart-specific protein FHL2 (35) is a reported AR coactivator that interacts with full-length AR but not with the NH_2- or COOH-terminal region (36), suggesting it recognizes an N/C interaction-induced conformation. The AR N/C interaction may contribute to the recognition of weaker androgen response elements whose regulation is androgen-specific (37).

Most steroid receptors undergo ligand-induced down-regulation resulting from ubiquitin-mediated proteolysis by the proteosome. Rates of receptor degradation have been correlated with activation potency (38), and activation domains and degradation signals can overlap (39). Proteosome-mediated degradation of estrogen receptor α (29, 40) was linked with coactivator recruitment and transcriptional potency. Mutations in the estrogen receptor α AF2 region at residues critical for coactivator recruitment stabilized the receptor (41), raising the possibility that p160 coactivator interaction with ligand-bound receptors is required for receptor degradation. The thyroid hormone receptor is also rapidly degraded by the proteosome (30), but ligand-dependent degradation of retinoid X receptor did not require transcriptional activity or interaction with p160 coactivators (42).

In our unpublished studies[2] AR degradation is mediated by the proteosome; however, in contrast to most nuclear receptors, AR and the vitamin D receptors (43) undergo agonist-induced stabilization. For the vitamin D receptor, inhibition of ubiquitin-proteosome-mediated degradation amplified the transcriptional response (43–45). For AR, it remains to be established whether *in vivo* transcriptional activity at certain androgen response elements requires the N/C interaction or the resulting agonist-induced increase in AR stability. The 5-fold reduced dissociation half-time of bound dexamethasone and reversal of the dexamethasone-induced decrease in GR levels in the TIF2-GR chimeras dramatically demonstrated the influence of the N/C interaction on receptor stabilization. This artificial N/C interaction in GR resulted in ligand dissociation and stability properties similar to those of wild-type AR.

[2] B. He and E. M. Wilson, unpublished material.

Dose-response transcription assays where TIF2 is transiently overexpressed as shown here indicate that the AR N/C interaction blocks AF2 recruitment of p160 coactivators. Transcriptional inhibition is predicted for other p160 coactivators such as SRC1 that interact with AF2 through L*XX*LL motifs. It is not known, however, to what extent inhibition of p160 coactivator recruitment by the N/C interaction limits the activity of these coactivators *in vivo*. Neither is it known how the interaction of other coactivators such as p300/CREB-binding protein or ARA70 with the AR is affected by the N/C interaction. Previous studies indicated that mutation of lysine 720 reduced the interaction of p160 coactivators with AF2, but this mutant AR retained full transcriptional activity (12). The corresponding lysine in mouse estrogen receptor α (lysine 366) was required for p160 coactivator recruitment and estrogen receptor α transcriptional activity (46).

p160 coactivator overexpression in transient transfection experiments (12) and possibly *in vivo* in some disease states (47) may increase steroid receptor transcriptional activity. This was shown for AR where coactivation by TIF2 was mediated by the AR NH_2-terminal and COOH-terminal regions (12, 48). However these types of studies do not address whether p160 coactivators increase AR activation when coactivators are present at normal physiological levels. We showed recently that TIF2 and SRC1 are almost undetectable in human benign hyperplastic prostatic tissue compared with greatly increased levels in recurrent prostate cancer (47). In recurrent prostate cancer, overexpression of p160 coactivators may effectively compete for the N/C interaction through their interaction with the NH_2- and COOH-terminal domains.

N/C interdomain interactions have been reported for other steroid and nuclear receptors; however, the potency and functional consequences differ. Intracellular phosphorylation of the A/B NH_2-terminal domain of PPAR-γ reduced ligand binding affinity (49). Interactions between the hinge-amino-terminal regions of the progesterone receptor contributed to dimerization and increased activation (50), whereas GR seems to lack an N/C interaction based on ligand dissociation (19) and direct interaction assays (51). Functional synergism between the NH_2- and COOH-terminal domains was also reported (52, 53). For estrogen receptor α and β, agonist-induced synergism was mediated by p300/CREB-binding protein and TIF2 binding to the NH_2-terminal region (54, 55). Similarly, in unpublished studies[2] we could not demonstrate direct NH_2- and COOH-terminal domain interactions for estrogen receptor α in glutathione *S*-transferase affinity matrix studies. CREB-binding protein and SRC1a were reported to enhance the AR N/C interaction through an indirect mechanism where coactivators act as adapters between activation function 1 and AF2 (56). The glutamine-rich region of SRC1e at residues 1053–1123 interacted with AR NH_2-terminal residues 360–494, suggesting SRC1 acts as a bridging molecule to mediate the N/C interaction (33). p160 coactivators also reportedly increased the AR N/C interaction, suggesting the N/C interaction is indirect. However, the identification of F*XX*LF and W*XX*LF motifs in the AR NH_2-terminal region (13) that bind the AF2 region of the ligand binding domain (12) provides strong evidence that the AR N/C interaction is direct. Moreover, transcriptional assays indicate that the agonist-induced N/C interaction interferes with the recruitment of p160 coactivators.

The AR F*XX*LF-AF2 N/C interaction is specific for the biologically active androgens testosterone and DHT and for anabolic steroids. However, the identification of the androgen-induced F*XX*LF-AF2 N/C interaction suggests that AR antagonists can be identified that inhibit or agonists that promote interactions with other F*XX*LF or L*XX*LL motif-containing proteins. Pharmaceutical ligands that bind AR with moderate or high affinity may promote interactions with related peptide sequences present in coregulatory proteins. Whether the F*XX*LF motif or related sequences occur in AR-specific coactivators that have sufficient affinity to compete for the agonist-induced N/C interaction or are induced to interact by other ligands remains to be established. In the presence of such ligands, coregulatory proteins might inhibit or compete for the androgen-induced N/C interaction to regulate tissue-selective AR-mediated gene activation.

Acknowledgments—We gratefully acknowledge the technical assistance of K. M. Cobb, D. Y. Zang, and L. W. Lee.

REFERENCES

1. Heery, D. M., Kalkhoven, E., Hoare, S., and Parker, M. G. (1997) *Nature* **387,** 733–736
2. McInerney, E. M., Rose, D. W., Flynn, S. E., Westin, S., Mullen, T. M., Krones, A., Inostroza, J., Torchia, J., Nolte, R. T., Assa-Munt, N., Milburn, M. V., Glass, C. K., and Rosenfeld, M. G. (1998) *Genes Dev.* **12,** 3357–3368
3. Voegel, J. J., Heine, M. J. S., Tini, M., Vivat, V., Chambon, P., and Gronemeyer, H. (1998) *EMBO J.* **17,** 507–519
4. Torchia, J., Rose, D. W., Inostroza, J., Kmei, Y., Westin, S., Glass, C., and Rosenfeld, M. (1997) *Nature* **382,** 677–684
5. Darimont, B. D., Wagner, R. L., Apriletti, J. W., Stallcup, M. R., Kushner, P. J., Baxter, J. D., Fletterick, R. J., and Yamamoto, K. R. (1998) *Genes Dev.* **12,** 3343–3356
6. Nolte, R. T., Wisely, G. B., Westin, S., Cobb, J. E., Lambert, M. H., Kurokawa, R., Rosenfeld, M. G., Willson, T. M., Glass, C. K., and Milburn, M. V. (1998) *Nature* **395,** 137–143
7. Matias, P. M., Donner, P., Coelho, R., Thomaz, M., Peixoto, C., Mecedo, S., Otto, N., Joschko, S., Scholz, P., Wegg, A., Basler, S., Schafer, M., Egner, U., and Carrondo, M. A. (2000) *J. Biol. Chem.* **275,** 26164–26171
8. Sack, J. S., Kish, K. F., Wang, C., Attar, R. M., Kiefer, S. E., An, Y., Wu, G. Y., Scheffler, J. E., Salvati, M. E., Krystek, S. R., Weinmann, R., and Einspahr, H. M. (2001) *Proc. Natl. Acad. Sci. U. S. A.* **98,** 4904–4909
9. Glass, C. K., Rose, D. W., and Rosenfeld, M. G. (1997) *Cur. Opin. Cell Biol.* **9,** 222–232
10. McKenna, N. J., Lanz, R. B., and O'Malley, B. W. (1999) *Endocr. Rev.* **20,** 321–344
11. Chen, H., Lin, R. J., Schiltz, R. L., Chakravarti, D., Nash, A., Nagy, L., Privalsky, M. L., Nakatani, Y., and Evans, R. M. (1997) *Cell* **90,** 569–580
12. He, B., Kemppainen, J. A., Voegel, J. J., Gronemeyer, H., and Wilson, E. M. (1999) *J. Biol. Chem.* **274,** 37219–37225
13. He, B., Kemppainen, J. A., and Wilson, E. M. (2000) *J. Biol. Chem.* **275,** 22986–22994
14. Kemppainen, J. A., Langley, E., Wong, C. I., Bobseine, K., Kelce, W. R., and Wilson, E. M. (1999) *Mol. Endocrinol.* **13,** 440–454
15. Langley, E., Kemppainen, J. A., and Wilson, E. M. (1998) *J. Biol. Chem.* **273,** 92–101
16. Langley, E., Zhou, Z. X., and Wilson, E. M. (1995) *J. Biol. Chem.* **270,** 29983–29990
17. Kraus, W. L., McInerney, E. M., and Katzenellenbogen, B. S. (1995) *Proc. Natl. Acad. Sci. U. S. A.* **92,** 12314–12318
18. Tetel, M. J., Giangrande, P. H., Leonhardt, S. A., McDonnell, D. P., and Edwards, D. P. (1999) *Mol. Endocrinol.* **13,** 910–924
19. Zhou, Z. X., Lane, M. V., Kemppainen, J. A., French, F. S., and Wilson, E. M. (1995) *Mol. Endocrinol.* **9,** 208–218
20. Voegel, J. J., Heine, M. J. S., Zechel, C., Chambon, P., and Gronemeyer, H. (1996) *EMBO J.* **15,** 3667–3675
21. Simental, J. A., Sar, M., Lane, M. V., French, F. S., and Wilson, E. M. (1991) *J. Biol. Chem.* **266,** 510–518
22. Onate, S. A., Tsai, S. Y., Tsai, M. J., and O'Malley, B. W. (1995) *Science* **270,** 1354–1357
23. Onate, S. A., Boonyaratanakornkit, V., Spencer, T. E., Tsai, S. Y., Tsai, M. J., Edwards, D. P., and O'Malley, B. W. (1998) *J. Biol. Chem.* **273,** 12101–12108
24. Anzick, S. L., Kononen, J., Walker, R. L., Azorsa, D. O., Tanner, M. M., Guan, X. Y., Sauter, G., Kallioniemi, O. P., Trent, J. M., and Meltzer, P. S. (1997) *Science* **277,** 965–968
25. Zegers, N. D., Claassen, E., Neelen, C., Mulder, E., van Laar, J. H., Voorhorst, M. M., Berrevoets, C. A., Brinkmann, A. O., van der Kwast, T. H., Ruizeveld de Winter, J. A. R., Trapman, J., and Boersma, W. J. A. (1991) *Biochim. Biophys. Acta* **1073,** 23–32
26. Zhou, Z. X., Wong, C. I., Sar, M., and Wilson, E. M. (1994) *Recent Prog. Horm. Res.* **49,** 249–274
27. Kemppainen, J. A., Lane, M. V., Sar, M., and Wilson, E. M. (1992) *J. Biol. Chem.* **267,** 968–974
28. Pakdel, F., Le Goff, P., and Katzenellenbogen, B. S. (1993) *J. Steroid Biochem. Mol. Biol.* **46,** 663–672
29. Nawaz, Z., Lonard, D. M., Dennis, A. P., Smith, C. L., and O'Malley, B. W. (1999) *Proc. Natl. Acad. Sci. U. S. A.* **96,** 1858–1862
30. Dace, A., Zhao, L., Park, K. S., Furuno, T., Takamura, N., Nakanishi, M., West, B. L., Hanover, J. A., and Cheng, S. Y. (2000) *Proc. Natl. Acad. Sci. U. S. A.* **97,** 8985–8990
31. Hoeck, W., Rusconi, S., and Groner, B. (1989) *J. Biol. Chem.* **264,** 14396–14402
32. Nardulli, A. M., and Katzenellenbogen, B. S. (1998) *Endocrinology* **122,** 1532–1540
33. Bevan, C. L., Hoare, S., Claessens, F., Heery, D. M., and Parker, M. G. (1999)

Mol. Cell. Biol. **19,** 8383–8392
34. Wang, Q., Lu, J. H., and Yong, E. L. (2001) *J. Biol. Chem.* **276,** 7493–7499
35. Chan, K. K., Tsui, S. K. W., Lee, S. M. Y., Luk, S. C. W., Liew, C. C., Fung, K. P., Waye, M. M. Y., and Lee, C. Y. (1998) *Gene* (*Amst.*) **210,** 345–350
36. Müller, J. M., Isele, U., Metzger, E., Rempel, A., Moser, M., Pscherer, A., Breyer, T., Holubarsch, C., Buettner, R., and Schüle, R. (2000) *EMBO J.* **19,** 359–369
37. Scheller, A., Hughes, E., Golden, K. L., and Robins, D. M. (1998) *J. Biol. Chem.* **273,** 24216–24222
38. Molinari, E., Gilman, M., and Nastesan, S. (1999) *EMBO J.* **18,** 6439–6447
39. Salghetti, S. E., Muratani, M., Wijnen, H., Futcher, B., and Tansey, W. P. (2000) *Proc. Natl. Acad. Sci. U. S. A.* **97,** 3118–3123
40. Alarid, E. T., Bakopoulos, N., and Solodin, N. (1999) *Mol. Endocrinol.* **13,** 1522–1534
41. Lonard, D. M., Nawaz, Z., Smith, C. L., and O'Malley, B. W. (2000) *Mol. Cell* **5,** 939–948
42. Osburn, D. L., Shao, G., Seidel, H. M., and Schulman, I. G. (2001) *Mol. Cell. Biol.* **21,** 4909–4918
43. Arbour, N. C., Prahl, J. M., and DeLuca, H. F. (1993) *Mol. Endocrinol.* **7,** 1307–1312
44. Li, X. Y., Boudjelal, M., Xiao, J. H., Peng, Z. H., Asuru, A., Kang, S., Fisher, G. J., and Voorhees, J. J. (1999) *Mol. Endocrinol.* **13,** 1686–1694
45. Santiso-Mere, D., Sone, T., Hilliard, G. M., Pike, J. W., and McDonnell, D. P. (1993) *Mol. Endocrinol.* **7,** 833–839
46. Henttu, P. M. A., Kalkhoven, E., and Parker, M. G. (1997) *Mol. Cell. Biol.* **17,** 1832–1839
47. Gregory, C. W., He, B., Johnson, R. T., Ford, O. H., Mohler, J. L., French, F. S., and Wilson, E. M. (2001) *Cancer Res.* **61,** 4315–4319
48. Alen, P., Claessens, F., Verhoeven, G., Rombauts, W., and Peeters, B. (1999) *Mol. Cell. Biol.* **19,** 6085–6097
49. Shao, D., Rangwala, S. M., Bailey, S. T., Krakow, S. L., Reginato, M. J., and Lazar, M. A. (1998) *Nature* **396,** 377–380
50. Tetel, M. J., Jung, S., Carbajo, P., Ladtkow, T., Skafar, D. F., and Edwards, D. P. (1997) *Mol. Endocrinol.* **11,** 1114–1128
51. Spanjaard, R. A., and Chin, W. W. (1993) *Mol. Endocrinol.* **7,** 12–16
52. McInerney, E. M., Tsai, M. J., O'Malley, B. W., and Katzenellenbogen, B. S. (1996) *Proc. Natl. Acad. Sci. U. S. A.* **93,** 10069–10073
53. Tasset, D., Tora, L., Fromental, C., Scheer, E., and Chambon, P. (1990) *Cell* **62,** 1177–1187
54. Kobayashi, Y., Kitamoto, T., Masuhiro, Y., Watanabe, M., Kase, T., Metzger, D., Yanagisawa, J., and Kato, S. (2000) *J. Biol. Chem.* **275,** 15645–15651
55. Benecke, A., Chambon, P., and Gronemeyer, H. (2000) *EMBO Rep.* **1,** 151–157
56. Ikonen, T., Palvimo, J. J., and Jänne, O. A. (1997) *J. Biol. Chem.* **272,** 29821–29828